渦法による疑似乱流の生成

Producing Artificial Turbulence by the Vortex Method

大上芳文、立命館大学、525-8577 草津市野路東 1-1-1、ogami@cfd.ritsumei.ac.jp
Yoshifumi Ogami, Ritsumeikan University, Noji-higashi, Kusatsu, Shiga 525-8577, Japan

A simple and accurate numerical method is presented to produce velocity fluctuations that are determined by the prescribed physical quantities and qualities of turbulence. The fluctuations are directly obtained by solving a system of nonlinear equations. This method requires as many computer memories and computations as one-dimensional case even for the three dimensional calculations. The solutions are quite accurate with less than 0.01% relative errors. Then these solutions are used to examine the capability of the vortex methods to produce turbulent flows with the prescribed parameters. Although the energy spectra by the vortex method scatter to some extent, they are distributed along the prescribed spectra even at the higher frequency regions. It can be said that the vortex methods are able to simulate the target turbulence qualitatively well. Also it is found that the solutions with the LES model increase and deviate from the target spectrum at the higher frequency regions.

1. INTRODUCTION

One of the crucial problems for the turbulent simulation is how to set up the inlet boundary condition that provides the physical quantities and qualities of turbulent flows as listed below.

1. Longitudinal and transverse spectra: $E_L(f)$ and $E_T(f)$
2. Root mean square of the velocity fluctuation: $\mathrm{RMS} = \sqrt{\frac{\int_0^T u(t)^2 dt}{T}}$
3. Mean velocity: U
4. Kinematic viscosity: ν
5. Longitudinal and transverse integral scale: L_{11} and L_{22}
6. Kolmogorov scale: $\eta = \left(\frac{2\nu^3 L_{11}}{u^3} \right)^{\frac{1}{4}}$
7. Gaussian frequency distribution of velocity fluctuations

Several researchers have presented numerical methods to produce velocity fluctuations for the turbulent simulation. Iwatani (1) used the multidimensional autoregressive processes to produce velocity fluctuations from the power spectra and the cross spectra of fluctuations. The velocity fluctuations are given by a linear summation of white noise and of the past fluctuations with the coefficients that are obtained by solving a system of linear equations. The simulated results are somewhat noisy and have to be modified to obtain desired RMS.

Maruyama and Morikawa (2), and Kondo et al. (3) used the method of the trigonometric series with Gaussian random coefficients, in which the velocity fluctuations are expressed by a series of cosine and sine functions. The coefficients of the functions are obtained by solving a system of linear equations. They do not consider the distant grid points to lighten computational loads. This may produce numerical errors that cannot be disregarded.

The first purpose of this paper is to present, in Section 2, a simpler and more accurate numerical method to produce series of velocity fluctuations. In this method, it is the longitudinal or transverse spectrum that is expressed by a series of cosine and sine functions. The coefficients of the functions are the velocity fluctuations themselves and these are obtained by solving a system of nonlinear (not linear) equations.

On the other hand, the vortex methods have been used for turbulent flow simulations with LES models (4, 5, 6, 7). Leonard and Chua (4), and Kiya and Izawa (5) incorporated the Smagorinsky model into the vortex methods by means of nonlinear core-spreading algorithm. Mansfield et al. (6) presented a LES scheme using a dynamic eddy diffusivity model. Kamemoto et al. (7) reviewed the recent works on LES modeling and emphasized the necessity of developing wall turbulence models. To see if these models are really working, it is necessary to examine whether the energy spectrum produced by these vortex methods are expected one because LES is to handle the energy spectrum of the lower frequency by modeling that of the higher frequency. Before doing this examination, it should be confirmed whether the vortex methods can handle the energy spectrum or are versatile enough to produce the prescribed energy spectrum. Totsuka and Obi (8) calculated the energy spectrum using vortices and reported that the spectrum deviates from the target at the higher frequency regions when the resolution (vortex number) is insufficient.

The next purpose of this paper is to examine the capability of the vortex methods to produce flows with the prescribed physical quantities and qualities of turbulence mentioned at the beginning of this section. To do so, in Section 3 we apply the results of Section 2 to the vortex methods, and the LES model is used to see how it works. It is found that the vortex methods are able to simulate the target turbulence qualitatively well, and that the solutions with the LES model increase and deviate from the target spectrum at the higher frequency regions.

2. PRODUCING VELOCITY FLUCTUATION

2.1 One-Dimensional Case

In this subsection, we introduce a method to numerically produce a series of velocity fluctuations, which are

determined by the prescribed physical quantities or parameters mentioned in Section 1.

We consider the following longitudinal spectrum $E_L(f)$ and the Eulerian time-correlation $R_E(\tau)$,

$$\begin{cases} E_L(f) = \overline{4u(t)^2}\int_0^T R_E(\tau)\cos(2\pi f\tau)\,d\tau \\ R_E(\tau) = \dfrac{\overline{u(t)\cdot u(t+\tau)}}{\overline{u(t)^2}} \end{cases} \tag{1}$$

In this case, the directions of the mean velocity U and the velocity fluctuation $u(t)$ are the same.

Equation (1) can be rewritten as

$$E_L(k) = \frac{4T}{N^2}\left[\sum_{j=0}^{N-1} u_j \cos\left(2\pi j\frac{k}{N}\right)\right]^2 + \frac{4T}{N^2}\left[\sum_{j=0}^{N-1} u_j \sin\left(2\pi j\frac{k}{N}\right)\right]^2 \tag{2}$$

where the following relations have been employed.

$$\begin{cases} \Delta t = \dfrac{T}{N}, \Delta f = \dfrac{1}{T}, t = j\Delta t = j\dfrac{T}{N}, \\ f = k\Delta f = \dfrac{k}{T} = \dfrac{k}{n\Delta t}, \\ f_{\max} = \dfrac{n}{2T} = \dfrac{1}{2\Delta t}\ \text{(Nyquist frequency)} \end{cases} \tag{3}$$

Equation (2) is regarded as a system of simultaneous quadratic equations with N unknowns, u_j. Since the number of the equations is $N/2$ ($k = 0 \sim N/2-1$), we divide Eq.(2) into two parts to supply the deficit in the equations as

$$\begin{cases} \dfrac{T}{N}\displaystyle\sum_{j=0}^{N-1} u_j \cos\left(2\pi j\frac{k}{N}\right) = \mathrm{sign}(r)\sqrt{\frac{T}{N}E_L(k)\frac{r^2}{r^2+1}} \\ \dfrac{T}{N}\displaystyle\sum_{j=0}^{N-1} u_j \sin\left(2\pi j\frac{k}{N}\right) = \mathrm{sign}(r)\sqrt{\frac{T}{N}E_L(k)\frac{1}{r^2+1}} \end{cases} \tag{4}$$

where r is a random number which we introduce expecting the frequency distribution of the solutions to be Gaussian. This division makes the equation number the same as the unknowns, and also linearizes the nonlinear equations, which promotes the convergence of the solutions.

When $k = 0$ for the lower equation in Eq.(4), all the coefficients in the left hand side become zero, which makes no sense. We use the following equation instead in order to incorporate RMS, which is given as one of the prescribed parameters.

$$\mathrm{RMS} = \sqrt{\frac{\displaystyle\sum_{j=0}^{N-1} {u_j}^2}{N}} \tag{5}$$

Equation (5) is nonlinear and thus the system of the simultaneous equations has to be treated as a nonlinear system. Even so, the velocity fluctuations can be obtained directly by as simple manner as just solving these equations because the unknowns are the velocity fluctuations themselves unlike the methods mentioned in Section 1 (1, 2, 3).

It should be noted that the solutions to the system of equations (4) and (5) are not unique so that various sets of

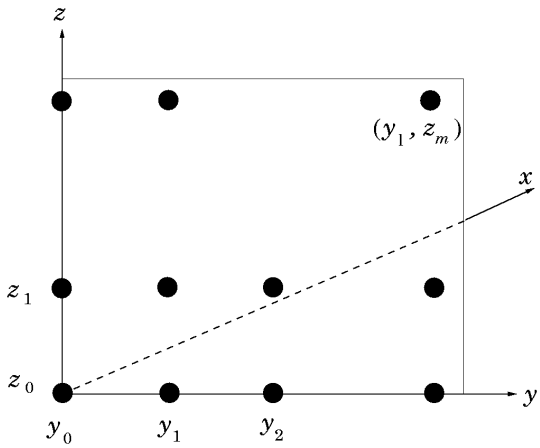

Figure 1 Three dimensional model

the solutions depending on the initial values and the random numbers can be obtained. This is another advantage of our method because of the coincidence with the characteristics of the turbulent flows.

2.2 Three-Dimensional Case

Since the inlet boundary is usually two-dimensional, the series of velocity fluctuations passing through the boundary grids must be produced on the basis of both the longitudinal correlation and of the transverse correlation.

As shown in Fig.1, we consider that the inlet boundary is located on the y-z plane, and that the fluid flows in the x- direction.

First, we obtain the velocity fluctuations u_j^{00} that pass through the grid point (y_0, z_0) by the method explained in subsection 2.1. Then the fluctuations u_j^{10} going through the next grid point (y_1, z_0) can be also obtained by the same procedure except that the following transverse correlation has to be incorporated.

$$\sum_{j=0}^{N-1}\frac{u_j^{00}u_j^{10}}{N} = \sum_{j=0}^{M/2-1}\frac{1}{T}E_T(k)\cos\left(2\pi\frac{k}{M}\right)$$

where $E_T(k)$ is the energy spectrum of the transverse correlation, and M is the grid number on the y- and z- axes. Further, the fluctuations u_j^{20} at the next point (y_2, z_0) require the following two more equations.

$$\sum_{j=0}^{N-1}\frac{u_j^{00}u_j^{20}}{N} = \sum_{j=0}^{M/2-1}\frac{1}{T}E_T(k)\cos\left(2\pi\frac{2k}{M}\right)$$

$$\sum_{j=0}^{N-1}\frac{u_j^{10}u_j^{20}}{N} = \sum_{j=0}^{M/2-1}\frac{1}{T}E_T(k)\cos\left(2\pi\frac{k}{M}\right)$$

Generally, the fluctuations u_j^{lm} at (y_l, z_m) are calculated by Eqs.(4) and (5), and the following equations

Table 1 Longitudinal and transverse correlations to consider

	x- direction	y- direction	z- direction
u	longitudinal	transverse	transverse
v	transverse	longitudinal	transverse
w	transverse	transverse	longitudinal

Table 2 Parameters used in simulation

Mean velocity: U	2.11m/s
Kinematic viscosity: ν	$1.562\times10^{-5}\mathrm{m}^2/\mathrm{s}$
Root mean square of velocity fluctuations: rms	0.159m/s
Time step: Δt	$1.94\times10^{-3}\mathrm{s}$
Grid spacing in flow direction: Δx	$U\Delta t$
Integral scale: L_{11}	$5\Delta x$
Fluctuation number: N	200
Grid number in x- and y- directions: M	20

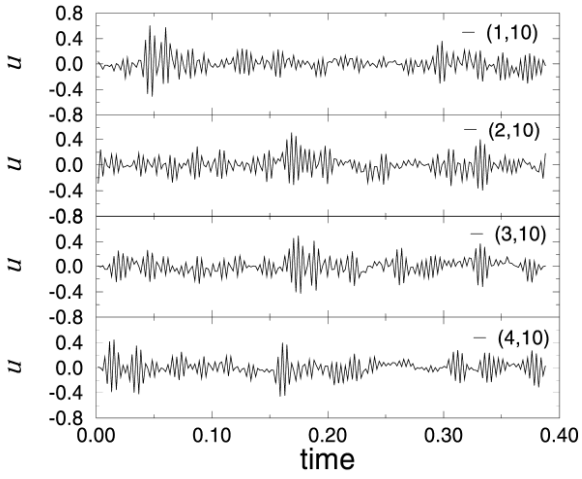

Figure 2 Calculated velocity fluctuations

$$\sum_{j=0}^{N-1}\frac{u_j^{l'm}u_j^{lm}}{N}=\sum_{j=0}^{M/2-1}\frac{1}{T}E_T(k)\cos\left(2\pi\frac{(l-l')k}{M}\right)\qquad(0\le l'<l)$$

$$\sum_{j=0}^{N-1}\frac{u_j^{lm'}u_j^{lm}}{N}=\sum_{j=0}^{M/2-1}\frac{1}{T}E_T(k)\cos\left(2\pi\frac{(m-m')k}{M}\right)\qquad(0\le m'<m)$$

The velocity fluctuations of the y- and z- components, v_j and w_j, can be obtained by the same procedures

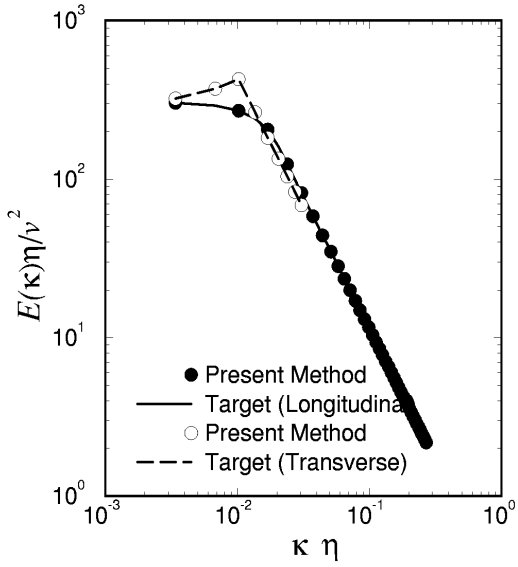

Figure 3 Target and calculated energy spectra

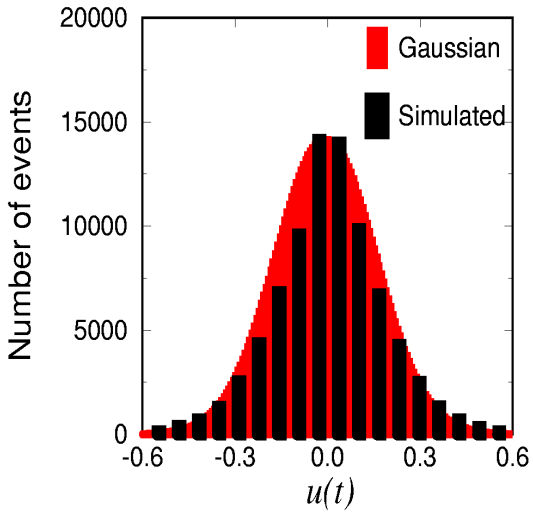

Figure 4 Frequency distribution

mentioned above except that the longitudinal correlation and the transverse correlation should be considered for each case (Table 1).

In this way, the velocity fluctuations on the inlet boundary are obtained from one grid to the next. The number of unknowns is always N regardless of the grid number M, and these are easily obtained by solving a system of nonlinear equations. This effectively saves the computer memories and loads.

2.3 Examples

For example simulations are conduced using the parameters listed in Table 2. The longitudinal and transverse spectra given in ref.(9) are used, and these spectra are illustrated in Fig.3 by the solid line (longitudinal) and by the dashed line (transverse). The system of nonlinear equations is solved by the subroutine "hybrd" provided in the free

Table 3 Parameters used in simulation

Mean velocity: U	10m/s
Kinematic viscosity: ν	$1.562\times10^{-5}\mathrm{m}^2/\mathrm{s}$
Root mean square of velocity fluctuations: rms	1.0m/s
Time step: Δt	$8.2\times10^{-4}\mathrm{s}$
Grid spacing in flow direction: Δx	$U\Delta t$
Integral scale: L_{11}	Δx and $30\Delta x$
Fluctuation number: N	1024
Grid number in y- and z- directions: M	2 and 1

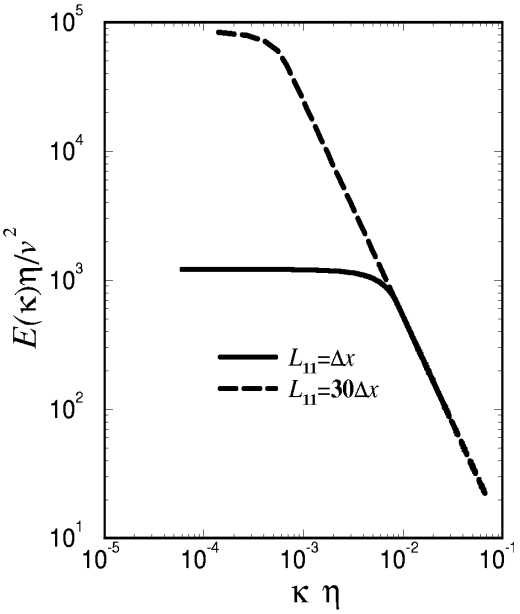

Figure 5 Target energy spectra

software package called minpac (downloadable at, for example, http://www.netlib.org/minpack/).

Figure 2 shows four examples of the simulated velocity fluctuations, which pass through the points (y_1, z_{10}), (y_2, z_{10}), (y_3, z_{10}) and (y_4, z_{10}). Though these are artificially produced, they resemble well those experimentally measured. Each series of the fluctuations is clearly different but the statistic is the same.

The spectra calculated from these fluctuations precisely agree with the target spectra as compared in Fig.3. The relative error is less than 0.01%, which can be controlled by the input parameter.

Figure 4 indicates that the velocity fluctuations are adequately random so that their frequency distribution fits the Gaussian distribution.

3. APPLICATION TO THE VORTEX METHOD

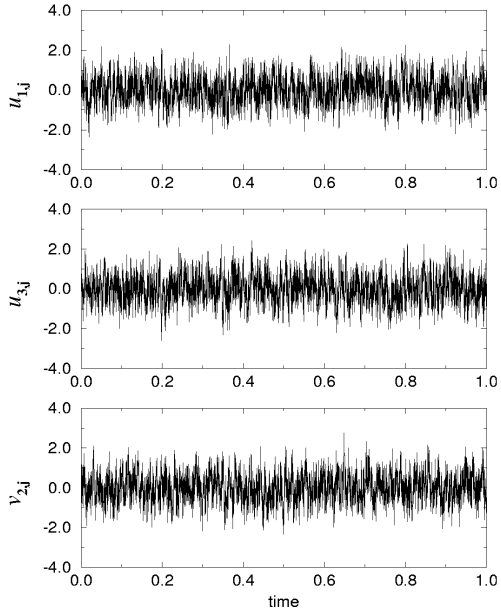

Figure 6 Velocity fluctuations at $L_{11} = \Delta x$

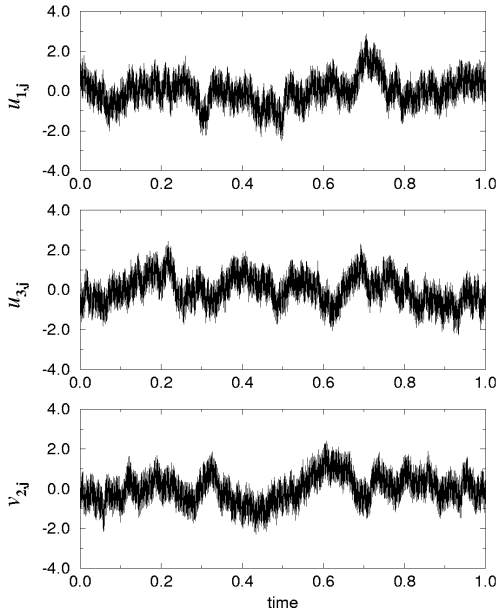

Figure 7 Velocity fluctuations at $L_{11} = 30\Delta x$

In this section, the capability of the vortex methods to produce flows with the prescribed physical quantities and qualities of turbulence is examined. Concretely, we examine whether the vortex methods can produce the prescribed longitudinal spectrum and the root mean square of the velocity fluctuations, and whether the frequency distribution is Gaussian.

3.1 Vortex Strength

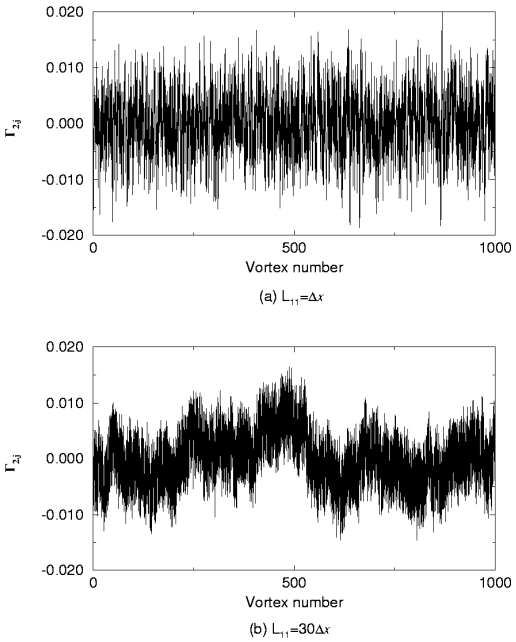

Figure 8 Vortex strength

Table 4 Parameters used in simulation

Mean velocity: U	10m/s
Kinematic viscosity: ν	$1.562\times10^{-5}\mathrm{m}^2/\mathrm{s}$
Time step: Δt	$8.2\times10^{-4}\mathrm{s}$
Initial core radius: σ	$2U\Delta t$
Updated core radius: σ '	$2\times$(distance to the nearest vortex)

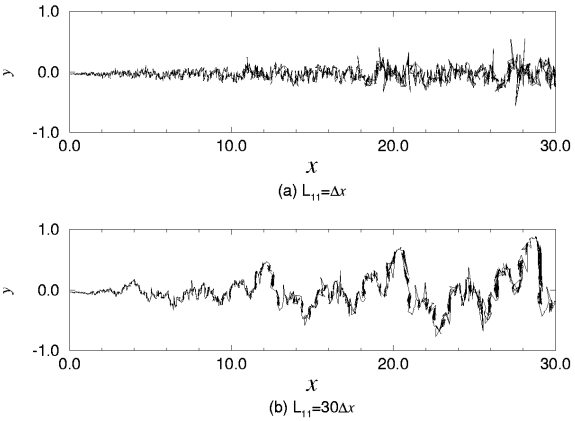

Figure 9 Vortex distributions

The velocity fluctuations produced in the previous section can be used as the boundary conditions of the finite-difference methods as well as the vortex methods as explained below.

In the two dimensional flows, the vortex strength is given by

$$\Gamma = \left(\frac{\partial v}{\partial x} - \frac{\partial u}{\partial y}\right)\Delta s \qquad (6)$$

where Δs is the area the vortex occupies. Using the velocity fluctuations u_j and v_j, Equation (6) can be approximately rewritten as

$$\Gamma_{j,l} = \left(\frac{v_{j+1,l} - v_{j-1,l}}{2\Delta x} - \frac{u_{j,l+1} - u_{j,l-1}}{2\Delta y}\right)\Delta s \qquad (7)$$

where the subscript j,l indicates the jth vortex or velocity fluctuation passing through the lth point on the y-axis.

Simulations are conducted for two different longitudinal integral scales, $L_{11} = \Delta x$ and $30\Delta x$ using the parameters listed in Table 3. The transverse spectrum is not considered for simplicity. The energy spectra obtained by these integral scales are illustrated in Fig.5 showing that the energy at smaller wave numbers increases with L_{11}.

Figures 6 and 7 show the velocity fluctuations respectively with $L_{11} = \Delta x$ and $30\Delta x$ which are calculated by the method explained in the previous section. Roughly speaking, the fluctuations of $L_{11} = \Delta x$ lie in the straight band while these of $L_{11} = 30\Delta x$ in the wavy band, which indicates that the latter fluctuations have more energy in the smaller wave number regions as the target spectrum (Fig.5).

The vortex strengths calculated using these fluctuations are shown in Fig.8. The characteristics of the vortex strength are very similar to that of the velocity fluctuations.

3.2 Vortex Methods and Turbulence

The vortices of the strengths calculated in subsection 3.1 are supplied at the origin one by one at each time step. The series of the strengths are used repeatedly until the simulations stop. We do not expect that the field of the velocity fluctuations (Figs.6, 7) can be completely reproduced by these vortices because of the use of limited number of the vortices.

The movements of the vortices are calculated by the vortex method with the diffusion velocity (10). The core radius of each vortex is updated to simulate the vortex stretch. The new core radius is $2\times$(distance to the nearest vortex). The parameters used for the simulations are listed in Table 4.

Figure 9 shows the vortex distributions at time 3.35872s, namely after supplying four cycles of the series of vortices. The successive vortices are connected by the straight lines. This figure is extended four times in the y-direction. It is observed that the arrangement of the vortices with $L_1 = 30\Delta x$ is much more wavy than the one with $L_1 = \Delta x$ just like the velocity fluctuations and the vortex strengths.

Figure 10 shows the velocity fluctuations at the point (20, 0) produced by the vortices. The velocity is zero until the vortices reach this point at almost time=2. The frequency distributions of these fluctuations shown in Fig.11 and 12 deviate somewhat from the Gaussian profile. The root mean square is 0.098m/s for $L_1 = \Delta x$ and 0.112m/s for

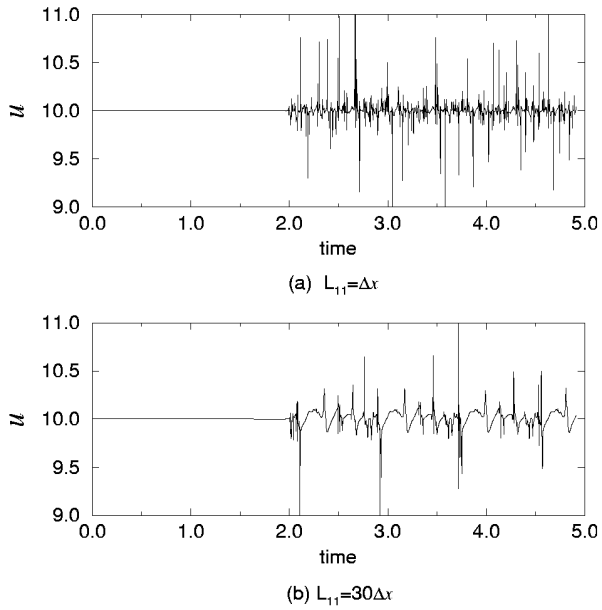

Figure 10 Velocity fluctuations produced by vortices

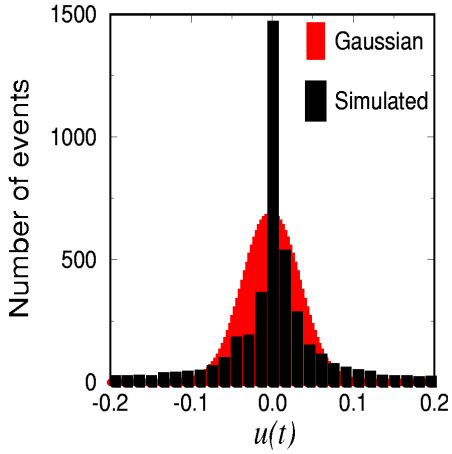

Figure 11 Frequency distribution by the vortex method $L_{11} = \Delta x$

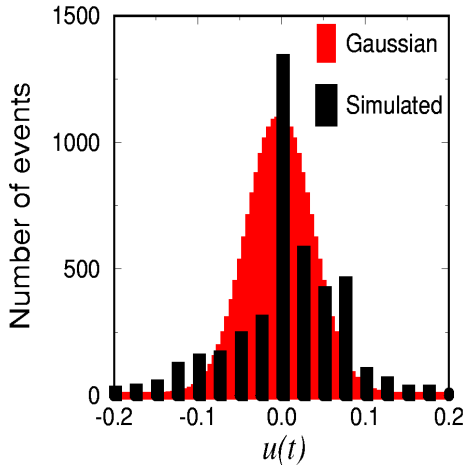

Figure 12 Frequency distribution by the vortex method $L_{11} = 30\Delta x$

L_1 ~~method~~ . These values are almost ten times smaller than

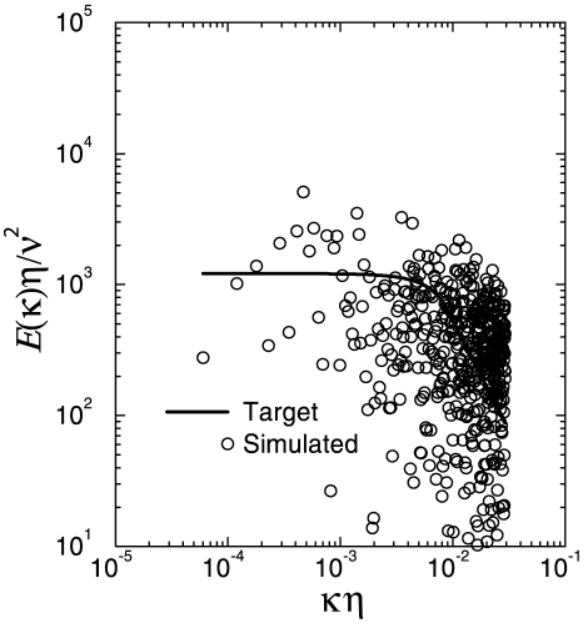

Figure 13 Target and simulated spectra with $L_{11} = \Delta x$

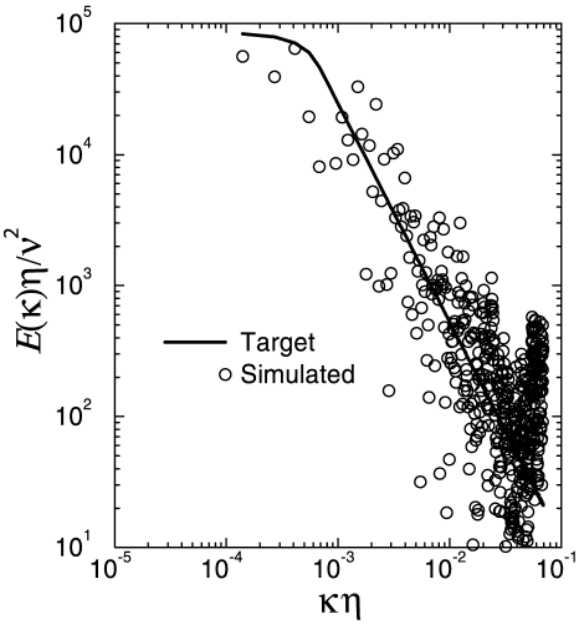

Figure 14 Target and simulated spectra with $L_{11} = 30\Delta x$

that in Table 3 (namely, 1.0m/s). This is because the vortex number is not large enough to reproduce the velocity fields (Figs. 6 and 7) with which the vortices are created.

The energy spectra calculated from these velocity fluctuations during t= 4.1984 ~ 5.03808 (namely, from 1024×5 steps to 1024×6 steps) are illustrated by the mark d in Figs.13 and 14. The energy spectrum is multiplied by E_V / E_T where E_V is the total energy of the spectrum by the vortex method and E_T is that of the target spectrum.

Though the calculated values are scattered to some extent, they are distributed surely along the target spectra even at the higher frequency regions in contrast to the results by Totsuka and Obi (8). We may say that qualitatively the vortex method can produce turbulent flows with prescribed parameters.

3.3 Vortex Methods and LES

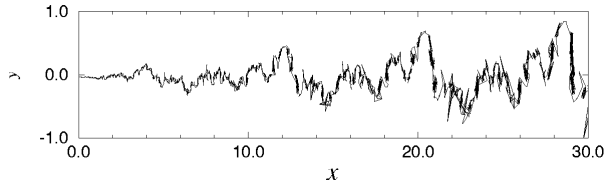

Figure 15 Vortex distribution with LES model

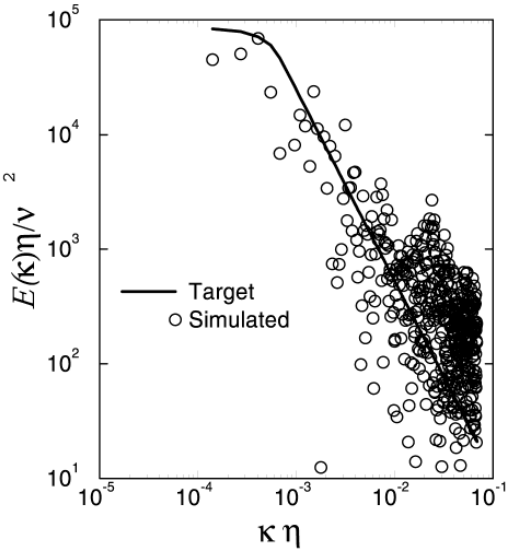

Figure 16 Energy spectrum with LES model (8)

The LES models for the vortex methods (4, 5) are used to see how they work. Simply, we add the subgrid scale viscosity

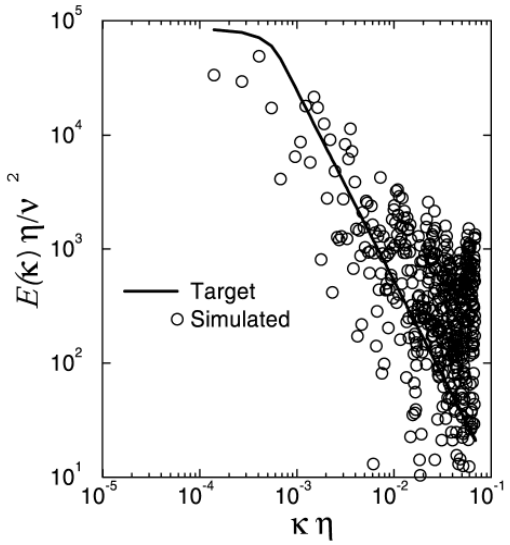

Figure 17 Energy spectrum with LES model (9)

$$\nu_{SGS} = \max\left[0, C^2\sigma^2 \frac{1}{\omega}\frac{d\omega}{dt}\right] \qquad (8)$$

adopted by Leonard and Chua, or

$$\nu_{SGS} = C^2\sigma^2 \frac{1}{\omega}\frac{d\omega}{dt} \qquad (9)$$

by Kiya et al. to the diffusion velocity. Here, C=0.17 is employed.

With the first model (8), the vortex distribution in Fig.15 is almost identical to the one without the model (Fig.9b). However, the spectrum at higher frequency regions slightly increases and deviates from the target as shown in Fig.16 because the LES model is to filter out the spectrum of higher frequency that the grid spacing cannot handle. With the second model (9), the spectrum at higher frequency regions deviates more from the target as shown in Fig.17. This may be because the subgrid scale viscosity can be smaller than zero, which never happens in the original LES model.

In contrast to the finite-difference methods, the grid spacing (the distances between vortices) of the vortex methods can increase and decrease freely so that we can obtain better solutions at the higher frequency regions (Fig.14) than those with the LES model (Fig.16).

4. CONCLUSION

First, a simple and accurate numerical method is presented to produce velocity fluctuations that are determined by the prescribed physical quantities and qualities of turbulence. The fluctuations are easily obtained by solving a system of nonlinear equations using free software. Also this method requires as many computer memories and computations as one-dimensional case even for the three dimensional calculations. The solutions are quite accurate with less than 0.01% relative errors.

Next, these fluctuations are used to examine the capability of the vortex methods to produce turbulent flows with the prescribed parameters. The RMS obtained is smaller than that expected probably because of the use of insufficient number of vortices. Although the energy spectra by the vortex method scatter to some extent, they are distributed along the prescribed spectra even at the higher frequency regions. It can be said that the vortex methods are able to simulate the target turbulence qualitatively well. Also the solutions with the LES model deviate from the target at the higher frequency regions. Further improvement will be required for obtaining quantitative agreement.

REFERENCES

(1) Iwatani, Y. (1982). "Simulation of multidimensional wind fluctuations having any arbitrary power spectra and cross spectra", Journal of Wind Engineering, No.11, p.5-18. (in Japanese)

(2) Maruyama, T. And Morikawa, H. (1994). "Numerical simulation of wind fluctuation conditioned by experimental data in turbulent boundary layer", Proc. 13th Symp. On Wind Eng., p.573-578. (in Japanese)

(3) Kondo, K. Murakami, S. And Mochida, A. (1997). "Generation of velocity fluctuations for inflow boundary condition of LES", Journal of Wind Engineering and Industrial Aerodynamics, Vol.67&68, p.51-64.

(4) Leonard, A. And Chua, K. (1989).

"Three-dimensional interactions of vortex tubes", Physica D, Vol.37, p.490-496.

(5) Kiya, M., Izawa, S. And Ishikawa, H. (1999). "Vortex method simulations of forced, impulsively started round jet", Proceedings of FEDSM'99, FEDSM99-6813.

(6) Mansfield, J.R., Knio, O.M. And Meneveau, C. (1999). "Dynamic LES of colliding vortex rings using a 3d vortex method", J. Comp. Phys., Vol.152, p.305-345.

(7) Kamemoto, K., Zhu, B. And Ojima, A. (2000). "Attractive features of an advanced vortex method and its subjects as a tool of lagrangian LES", Proceedings of 14th Symposium of Computational Fluid Dymanics, B06-4.

(8) Totsuka, Y. And Obi, S. (2000). "Turbulent flow analysis by a three dimensional vortex method (estimation of the dissipation rate)", Proceedings of 14th Symposium of Computational Fluid Dymanics, E09-4 (in Japanese)

(9) Tennekes, H. And Lumley, J.L. (1999). A First Course in Turbulence, 17th edn., MIT Press, Cambridge, p.273.

(10) Ogami, T. And Akamatsu, T. (1991). "Viscous flow simulation using the discrete vortex method – the diffusion velocity method", Computers & Fluids, Vol.19, p.433-441.